Stochastic resonance driven by two different kinds of colored noise in a bistable system

Xiaoqin Luo and Shiqun Zhu*
China Center of Advanced Science and Technology (World Laboratory), P.O. Box 8730, Beijing 100080, People's Republic of China and Department of Physics, College of Sciences, Suzhou University, Suzhou, Jiangsu 215006, People's Republic of China

(Received 1 April 2002; revised manuscript received 22 October 2002; published 13 February 2003)

The phenomenon of stochastic resonance in a bistable nonlinear system is investigated when both the multiplicative noise and the coupling between additive and multiplicative noise are colored with different values of noise correlation time τ_1 and τ_2. Combining the functional analysis and unified colored noise approximation, the two different kinds of colored noise in the nonlinear system can be simplified. The signal-to-noise ratio is calculated when a weakly periodic signal is added to the system. It is found that there appears a transition between one peak and two peaks in the curve of the signal-to-noise ratio when either the noise correlation time τ_1 and τ_2 or the coupling strength λ between additive and multiplicative noise is increased. The transition between one and two peaks depending on τ_1 and λ is more complex than that depending on τ_2.

DOI: 10.1103/PhysRevE.67.021104 PACS number(s): 05.40.−a, 02.50.−r

I. INTRODUCTION

In recent years, the phenomenon of stochastic resonance (SR) in nonlinear systems has been investigated extensively both theoretically and experimentally due to its potential applications [1–24]. The output signal of the nonlinear system may be amplified in the presence of an optimal level of noise and a weak periodic signal. The SR phenomenon appears in many fields, such as periodically recurrent of ice ages [1,2], electronic and magnetic systems [3,4], etc. Recently, there have appeared some extensions of SR, such as double SR [24,25], stochastic multiresonance [26–30], quantum SR [31], superthreshold SR [32,33], control of SR [34–37], etc.

In general, the multiplicative noise and additive noise of a nonlinear system are taken as different origins. But in certain situations both multiplicative and additive noise may have a common origin and then may be coupled as well. Two coupled noise sources were discussed for a two-dimensional hydrodynamical problem [38,39]. Meanwhile, in most of the previous analysis concerning the phenomenon of SR, only white noise is considered. However, the colored nature of the noise can also play an important role in the system.

In this paper, the SR phenomenon in a bistable system with coupling between multiplicative and additive noise is investigated when the multiplicative noise and the coupling between two noise terms are colored with nonzero correlation time τ_1 and τ_2. In Sec. II, the two different kinds of colored noise in the system are simplified when the functional analysis and unified colored noise approximation (UCNA) are employed. Then the expression of the signal-to-noise ratio (SNR) is derived. In Sec. III, the effects of multiplicative colored noise correlation time τ_1, noise correlation time τ_2 of the coupling between two noise terms, the coupling strength λ, and the signal frequency Ω on SNR are discussed. In Sec. IV, the numerical simulation is presented to check the validity of the approximation method. The spectral power amplification (SPA) is compared to the SNR. In Sec. V, the transition between one peak and two peaks in the SNR is presented on the parameter planes of τ_1-Ω, τ_2-Ω, and λ-Ω. A discussion of the effects concludes the paper.

*Corresponding author. Mailing address: Department of Physics, College of Sciences, Suzhou University, Suzhou, Jiangsu 215006, People's Republic of China.

II. THEORETICAL ANALYSIS

If a nonlinear system contains colored noise, it is a non-Markov stochastic process. It is necessary to develop some approximate methods to transform the non-Markov process to the Markov process in order to get analytic results. The functional analysis and the UCNA are the methods commonly used in the analysis [16,40–43].

A. Simplification of two different kinds of colored noise

The nonlinear stochastic system with both colored and white noise follows the Langevin equation

$$\frac{dx}{dt}=h(x)+g_1(x)\xi(t)+g_2(x)\eta(t), \tag{1}$$

where $h(x)$ is the deterministic part, and $g_1(x)$ and $g_2(x)$ are coefficients of colored noise $\xi(t)$ and white noise $\eta(t)$, respectively. The two noise terms are characterized by their mean and variance

$$\begin{aligned}
&\langle \xi(t)\rangle=\langle \eta(t)\rangle=0,\\
&\langle \xi(t)\xi(t')\rangle=\frac{P'}{\tau_1}\exp\left[-\frac{|t-t'|}{\tau_1}\right],\\
&\langle \eta(t)\eta(t')\rangle=2P\delta(t-t'),\\
&\langle \xi(t)\eta(t')\rangle=\langle \eta(t)\xi(t')\rangle=\frac{\lambda\sqrt{PP'}}{\tau_2}\exp\left[-\frac{|t-t'|}{\tau_2}\right].
\end{aligned} \tag{2}$$

Here τ_1 and P' are the correlation time and intensity of the multiplicative colored noise, respectively. P is the intensity of white noise, and τ_2 is the noise correlation time of the coupling between multiplicative and additive noise.

In the limit $\tau_1 \to 0$, the multiplicative noise tends to white noise, while the coupling between multiplicative and additive noise is colored correlated. According to the stochastic Liouville equation, Eq. (1) satisfies

$$\frac{\partial Q(x,t)}{\partial t}=-\frac{\partial}{\partial x}h(x)Q(x,t)-\frac{\partial}{\partial x}g_1(x)\langle\xi(t)\delta(x(t)-x)\rangle-\frac{\partial}{\partial x}g_2(x)\langle\eta(t)\delta(x(t)-x)\rangle. \tag{3}$$

Here the probability distribution function can be expressed as $Q(x,t)=\langle\delta(x(t)-x)\rangle$.

By applying the Novikov theorem and Fox's approach [16,40,42,43], the approximate Fokker-Planck equation corresponding to Eq. (3) can be written as

$$\frac{\partial Q(x,t)}{\partial t}=-\frac{\partial}{\partial x}h(x)Q(x,t)+P'\frac{\partial}{\partial x}g_1(x)\frac{\partial}{\partial x}g_1(x)Q(x,t)+\frac{\lambda\sqrt{PP'}}{1-\tau_2\left[h'(x_s)-\frac{g_2'(x_s)}{g_2(x_s)}h(x_s)\right]}\frac{\partial}{\partial x}\times g_1(x)\frac{\partial}{\partial x}g_2(x)Q(x,t)+P\frac{\partial}{\partial x}g_2(x)\frac{\partial}{\partial x}g_2(x)Q(x,t)+\frac{\lambda\sqrt{PP'}}{1-\tau_2\left[h'(x_s)-\frac{g_1'(x_s)}{g_1(x_s)}h(x_s)\right]}\frac{\partial}{\partial x}\times g_2(x)\frac{\partial}{\partial x}g_1(x)Q(x,t). \tag{4}$$

If the multiplicative noise is colored with finite correlation time τ_1, the UCNA method can be employed [16,20,40,41]. Thus the non-Markov process of Eq. (1) can be simplified to a one-dimensional Markov process

$$\frac{dx}{dt}=\frac{1}{A(x,\tau_1)}[h(x)+g_1(x)\Gamma(t)+g_2(x)\eta(t)], \tag{5}$$

with

$$A(x,\tau_1)=1-\tau_1\left[h'(x)-\frac{g_1'(x)}{g_1(x)}h(x)\right]. \tag{6}$$

Here $h'(x)$ and $g_1'(x)$ are the derivatives of $h(x)$ and $g_1(x)$ with respect to x and $\Gamma(t)$ is white noise with

$$\langle\Gamma(t)\rangle=0,\quad \langle\Gamma(t)\Gamma(t')\rangle=2P'\delta(t-t'). \tag{7}$$

By combining the results, Eq. (4), of the functional analysis and Eq. (5) of the UCNA, the Fokker-Planck equation corresponding to Eqs. (1) and (2) can be written as

$$\frac{\partial Q(x,t)}{\partial t}=-\frac{\partial}{\partial x}\frac{h(x)}{A(x,\tau_1)}Q(x,t)+P'\frac{\partial}{\partial x}\frac{g_1(x)}{A(x,\tau_1)}\frac{\partial}{\partial x}\frac{g_1(x)}{A(x,\tau_1)}Q(x,t)+\frac{\lambda\sqrt{PP'}}{1-\frac{\tau_2}{A(x_s,\tau_1)}\left[h'(x_s)-\frac{g_2'(x_s)}{g_2(x_s)}h(x_s)\right]}\frac{\partial}{\partial x}\frac{g_1(x)}{A(x,\tau_1)}\frac{\partial}{\partial x}\frac{g_2(x)}{A(x,\tau_1)}Q(x,t)+P\frac{\partial}{\partial x}\frac{g_2(x)}{A(x,\tau_1)}\frac{\partial}{\partial x}\frac{g_2(x)}{A(x,\tau_1)}Q(x,t)+\frac{\lambda\sqrt{PP'}}{1-\frac{\tau_2}{A(x_s,\tau_1)}\left[h'(x_s)-\frac{g_1'(x_s)}{g_1(x_s)}h(x_s)\right]}\frac{\partial}{\partial x}\frac{g_2(x)}{A(x,\tau_1)}\frac{\partial}{\partial x}\frac{g_1(x)}{A(x,\tau_1)}Q(x,t). \tag{8}$$

Thus the two different kinds of colored noise can be approximated and expressed by Eq. (8).

It should be mentioned that the regime of the approximation method used in deriving Eq. (8) is [40]

$$G(x,\tau_1,\tau_2)=\left\{1-\frac{\tau_2}{A(x,\tau_1)}\left[h'(x_s)-\frac{g_1'(x_s)}{g_1(x_s)}h'(x_s)\right]\right\}>0, \tag{9}$$

$$G(x,\tau_1,\tau_2)\gg\lambda\sqrt{PP'}\left|\frac{h'(x)}{h(x)}\right|.$$

In the following calculations, these conditions are satisfied.

B. Steady-state distribution function of a bistable system

When a weak periodic signal is added to a bistable system with coupling between multiplicative colored noise and additive white noise, the system follows the Langevin equation

$$\frac{dx}{dt}=-V'(x)+x\xi(t)+\eta(t)+\varepsilon\cos\Omega t, \tag{10}$$

where $V'(x)$ is the derivative of the symmetric potential $V(x)=-x^2/2+x^4/4$ with respect to x, which has two stable states at $x_\pm=\pm1$ and an unstable state at $x_u=0$. Meanwhile,

$h(x)=-V'(x)+\varepsilon\cos\Omega t$, $g_1(x)=x$, $g_2(x)=1$, and $\xi(t)$, $\eta(t)$ have the same characteristics as that in Eqs. (2) and (3). From Eq. (4), one has

$$\frac{\partial Q(x,t)}{\partial t}=-\frac{\partial}{\partial x}[h(x)+g'(x)g(x)]Q(x,t)+\frac{\partial^2}{\partial x^2}g(x)g(x)Q(x,t), \tag{11}$$

where

$$g(x)=\left[P'g_1^2(x)+\frac{2\lambda\sqrt{PP'}}{1+2\tau_2}g_1(x)g_2(x)+Pg_2^2(x)\right]^{1/2}. \tag{12}$$

According to Eqs. (6), (10), and (12), one has

$$A(x,\tau_1)=1+2\tau_1x^2+\frac{\tau_1\varepsilon\cos\Omega t}{x},$$

$$g(x)=\left[P'x^2+\frac{2\lambda\sqrt{PP'}}{1+2\tau_2}x+P\right]^{1/2}. \tag{13}$$

Thus the corresponding Fokker-Planck equation of the bistable system, Eq. (10), can be written as

$$\frac{\partial Q(x,t)}{\partial t}=-\frac{\partial}{\partial x}F(x,\tau_1,\tau_2,\lambda)Q(x,t)+\frac{\partial^2}{\partial x^2}D(x,\tau_1,\tau_2,\lambda)Q(x,t), \tag{14}$$

in which

$$F(x,\tau_1,\tau_2,\lambda)=\tilde{h}(x)+\tilde{g}(x)\frac{d\tilde{g}(x)}{dx},$$

$$D(x,\tau_1,\tau_2,\lambda)=\tilde{g}^2(x), \tag{15}$$

with

$$\tilde{h}(x)=\frac{h(x)}{A(x,\tau_1)},\quad \tilde{g}(x)=\frac{g(x)}{A(x,\tau_1)}.$$

Since the frequency Ω is very small, there is enough time for the system to reach the local equilibrium during the period of $1/\Omega$. Then the quasi-steady-state distribution function $Q_s(x,t)$ can be derived from Eqs. (13)–(15) in the adiabatic limit:

$$Q_s(x,t)=\left[\frac{A(x,\tau_1)}{g(x)}\right]\exp\left[\int\frac{h(x)A(x,\tau_1)}{g^2(x)}dx\right]=\left[\frac{A(x,\tau_1)}{g(x)}\right]\exp\left[-\frac{\Phi(x)}{P'}\right]. \tag{16}$$

Here $\Phi(x)$ is the rectified potential function and its form follows

$$\begin{aligned}\Phi(x)={}&\frac{\tau_1}{2}x^4-\frac{4\lambda\tau_1}{3(1+2\tau_2)}\sqrt{\frac{P}{P'}}x^3+\alpha_1x^2+\alpha_2x\\&+\beta\ln\left[P'x^2+\left(\frac{2\lambda\sqrt{PP'}}{1+2\tau_2}\right)x+P\right]\\&+\frac{\gamma_1}{\sqrt{1-\lambda^2/(1+2\tau_2)^2}}\\&\times\arctan\left[\frac{\sqrt{P'/P}x+\lambda/(1+2\tau_2)}{\sqrt{1-\lambda^2/(1+2\tau_2)^2}}\right]\\&+\left\{-\tau_1x+\frac{\lambda\tau_1}{1+2\tau_2}\sqrt{\frac{P}{P'}}\right.\\&\times\ln\left[P'x^2+\frac{2\lambda\sqrt{PP'}}{1+2\tau_2}x+P\right]-\frac{\gamma_2}{\sqrt{1-\lambda^2/(1+2\tau_2)^2}}\\&\left.\times\arctan\left[\frac{\sqrt{P'/P}x+\lambda/(1+2\tau_2)}{\sqrt{1-\lambda^2/(1+2\tau_2)^2}}\right]\right\}\varepsilon\cos\Omega t,\end{aligned} \tag{17}$$

where

$$\alpha_1=\frac{P}{P'}\tau_1\left[4\left(\frac{\lambda}{1+2\tau_2}\right)^2-1\right]-\frac{2\tau_1-1}{2},$$

$$\alpha_2=8\sqrt{\left(\frac{P}{P'}\right)^3}\left(\frac{\lambda\tau_1}{1+2\tau_2}\right)\left[1-2\left(\frac{\lambda}{1+2\tau_2}\right)^2\right]+2\sqrt{\frac{P}{P'}}\left[\frac{\lambda(2\tau_1-1)}{1+2\tau_2}\right],$$

$$\beta=-\frac{1}{2}-\frac{P}{2P'}(2\tau_1-1)\left[4\left(\frac{\lambda}{1+2\tau_2}\right)^2-1\right]+\left(\frac{P}{P'}\right)^2\tau_1\left\{16\left(\frac{\lambda}{1+2\tau_2}\right)^4-12\left(\frac{\lambda}{1+2\tau_2}\right)^2+1\right\},$$

$$\begin{aligned}\gamma_1={}&\frac{\lambda}{1+2\tau_2}+\frac{P}{P'}\left[\frac{\lambda(2\tau_1-1)}{1+2\tau_2}\right]\left[4\left(\frac{\lambda}{1+2\tau_2}\right)^2-3\right]\\&+2\left(\frac{P}{P'}\right)^2\left(\frac{\lambda\tau_1}{1+2\tau_2}\right)\left\{-16\left(\frac{\lambda}{1+2\tau_2}\right)^4\right.\\&\left.+20\left(\frac{\lambda}{1+2\tau_2}\right)^2-5\right\},\end{aligned} \tag{18}$$

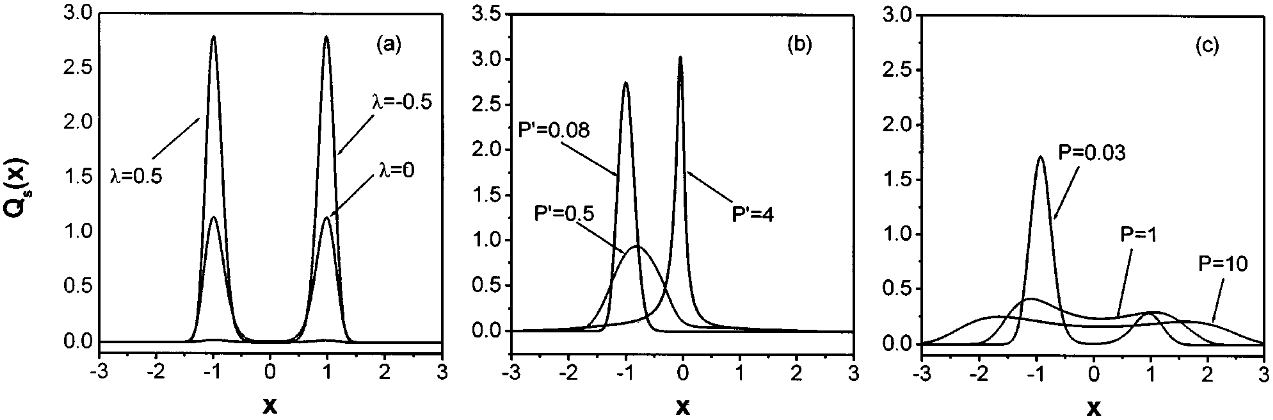

FIG. 1. Quasi-steady-state probability density function $Q_s(x)$ as a function of the variable x, the coupling constant λ, and the noise correlation time τ_1 and τ_2. All parameters are dimensionless. (a) The $Q_s(x)$ is plotted when $\lambda=-0.5$, 0, 0.5. The parameters are chosen as $\tau_1=0.5$, $\tau_2=0.2$, $\varepsilon=0$, $\omega=0.002$, $P=0.03$, and $P'=0.08$. (b) The $Q_s(x)$ is plotted when $P'=0.08$, 0.5, 4. The parameters are chosen as $\lambda=0.5$, $\tau_1=0.4$, $\tau_2=0.2$, $\varepsilon=0.05$, $\omega=0.002$, and $P=0.03$. (c) The $Q_s(x)$ is plotted when $P=0.03$, 1, 10. The parameters are chosen as $\lambda=0.5$, $\tau_1=0.1$, $\tau_2=0.2$, $\varepsilon=0.05$, $\omega=0.0015$, and $P'=0.08$.

$$\gamma_2=\sqrt{\frac{P'}{P}}(\tau_1+1)+\sqrt{\frac{P}{P'}}\tau_1\left[2\left(\frac{\lambda}{1+2\tau_2}\right)^2-1\right].$$

The quasi-steady-state probability density function (PDF) $Q_s(x)$ of Eq. (16) is plotted in Fig. 1 as a function of the variable x when the parameters of the coupling constant λ and multiplicative and additive noise strengths P' and P are varied.

The PDF of $Q_s(x)$ is plotted in Fig. 1(a) when the coupling constant λ is varied and there is no signal with $\varepsilon=0$. It is seen that the peak in $Q_s(x)$ is shifted from $x=+1$ to $x=-1$ when λ is changed from -0.5 to $+0.5$. When $\lambda=0$, there are two peaks in $Q_s(x)$ with the same height and width. When there is a signal with $\varepsilon>0$, similar shape in $Q_s(x)$ is obtained. The two-peak structure appearing in PDF depends on the value of λ.

The PDF of $Q_s(x)$ is plotted in Fig. 1(b) when the multiplicative noise strength P' is varied with $\lambda=0.5$. It is seen that the peak in $Q_s(x)$ at $x=-1$ is decreased and then shifted to $x=0$ when the value of P' is increased from 0.08 to 4. For $\lambda=-0.5$, similar behavior is obtained. The peak in $Q_s(x)$ at $x=+1$ is decreased and then shifted to $x=0$ when P' is increased.

The PDF of $Q_s(x)$ is plotted in Fig. 1(b) when the additive noise strength P is varied with $\lambda=0.5$. It is seen that there are two peaks in $Q_s(x)$ located at $x=-1$ and $+1$. The peak located at $x=-1$ is much higher than that at $x=+1$ when $P=0.03$. When P is increased to 10, the curve of $Q_s(x)$ is widened and the left peak is decreased with almost the same height to the right one. The locations of the two peaks are shifted to nearly $x=-1.7$ and $+1.7$. When $\lambda=-0.5$, similar behavior is observed. The peak in $Q_s(x)$ located at $x=+1$ is much higher for a small value of P. The two peaks are almost with same height when P is very large.

From Figs. 1(a)–1(c), it is seen that the $Q_s(x)$ with two peaks of the same height is symmetrically located about $x=0$ when the coupling $\lambda=0$. When $\lambda\neq0$, the symmetry is broken. There appears either only one peak or two peaks with quite different heights.

C. Signal-to-noise ratio

The expression of the SNR, $\mathcal{R}$, in the bistable system can be derived from the two-state approach with two stable states ($x_\pm$) and given by [3,16]

$$\mathcal{R}=\frac{\pi W_1^2\varepsilon^2}{4W_0}\left[1-\frac{W_1^2\varepsilon^2}{2(W_0^2+\Omega^2)}\right]^{-1}, \tag{19}$$

where

$$W_0=\left(\frac{\sqrt{2}a}{\pi}\right)\exp\left[\frac{1}{P'}\left\{E_{1\pm}+\beta\ln\left(\frac{P'}{P}\pm2\sqrt{\frac{P'}{P}}\times\left(\frac{\lambda}{1+2\tau_2}\right)+1\right)+\gamma_1B_1(\lambda,\tau_2)\right\}\right], \tag{20}$$

$$W_1=E_2W_0$$

and

$$E_{1\pm}=\frac{1-\tau_1}{2}+\frac{P\tau_1}{P'}\left[4\left(\frac{\lambda}{1+2\tau_2}\right)^2-1\right]\mp\frac{4}{3}\sqrt{\frac{P}{P'}}\left(\frac{\lambda\tau_1}{1+2\tau_2}\right)\pm\left\{8\sqrt{\left(\frac{P}{P'}\right)^3}\left(\frac{\lambda\tau_1}{1+2\tau_2}\right)\left[1-2\left(\frac{\lambda}{1+2\tau_2}\right)^2\right]+2\sqrt{\frac{P}{P'}}\left[\frac{\lambda(2\tau_1-1)}{1+2\tau_2}\right]\right\},$$

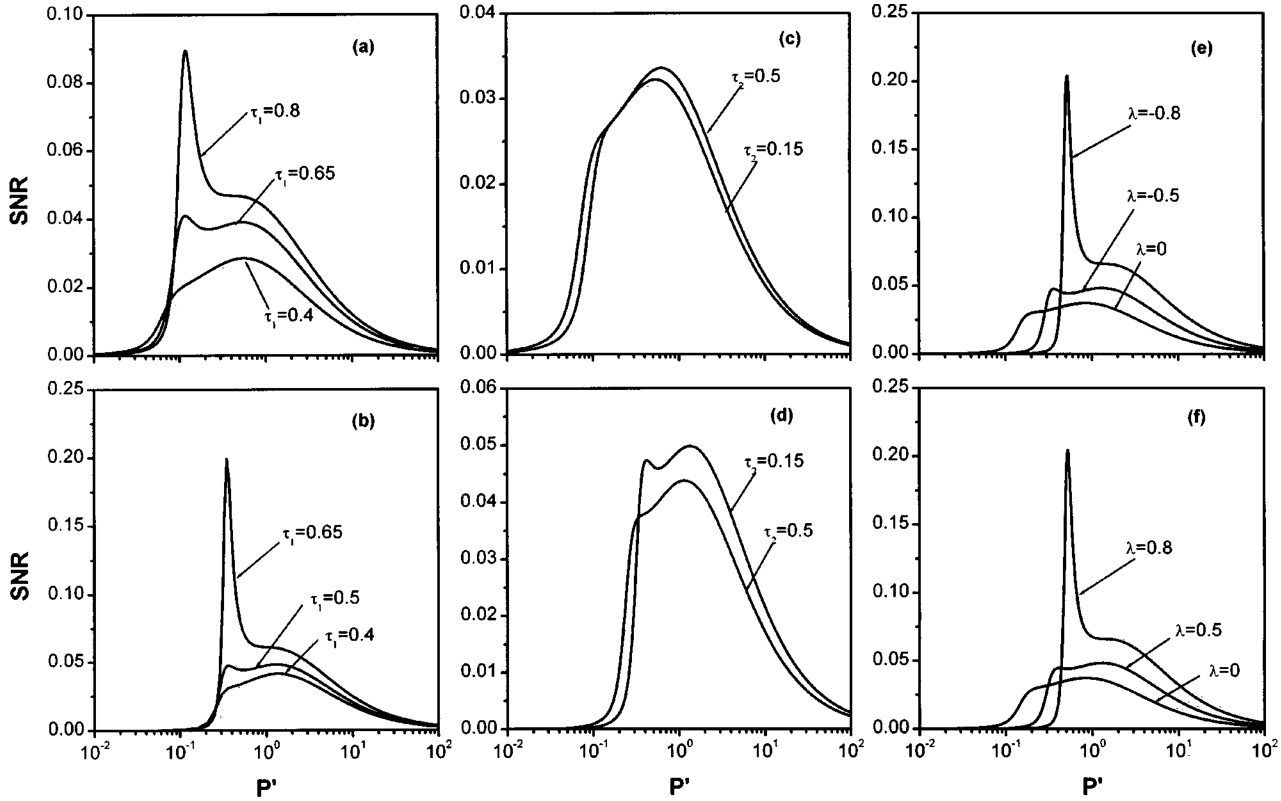

FIG. 2. Signal-to-noise ratio is as a function of the multiplicative noise intensity P'. The parameters are chosen as follows: $P=0.03$ and $\varepsilon=0.05$. All parameters are dimensionless. (a), (c), and (e) The initial condition is $x(0)=x_+$. (b), (d), and (f) The initial condition is $x(0)=x_-$. (a) and (b) The values of the multiplicative noise correlation time τ_1 are different. $\lambda=0.5$, $\tau_2=0.2$, and $\Omega=0.002$. (c) and (d) The values of the correlation time τ_2 of the coupling between two noise terms are different. $\lambda=0.5$, $\tau_1=0.5$, and $\Omega=0.0023$. (e) and (f) The values of the coupling strength λ are different. $\tau_1=0.5$, $\tau_2=0.2$, and $\Omega=0.002$.

$$B_1(\lambda,\tau_2)=\frac{1}{\sqrt{1-\lambda^2/(1+2\tau_2)^2}}\left\{\arctan\left[\frac{\frac{\lambda}{1+2\tau_2}\pm\sqrt{\frac{P'}{P}}}{\sqrt{1-\lambda^2/(1+2\tau_2)^2}}\right]-\arctan\left[\frac{\lambda/(1+2\tau_2)}{\sqrt{1-\lambda^2/(1+2\tau_2)^2}}\right]\right\},$$

$$E_2=\frac{\gamma_2 B_1(\lambda,\tau_2)\pm\tau_1-\sqrt{\frac{P}{P'}}\left(\frac{\lambda\tau_1}{1+2\tau_2}\right)\ln\left[\frac{P'}{P}\pm 2\sqrt{\frac{P'}{P}}\left(\frac{\lambda}{1+2\tau_2}\right)+1\right]}{P'},\tag{21}$$

and β, γ_1, and γ_2 are the same as in Eq. (18).

III. EFFECTS OF NOISE CORRELATION TIME τ_1, τ_2 AND COUPLING STRENGTH λ ON STOCHASTIC RESONANCE

By virtue of Eqs. (19)–(21), the SNR in the bistable system can be easily calculated as functions of different parameters.

A. Multiplicative noise

The SNR as a function of the multiplicative noise intensity P' is plotted in Fig. 2 for different values of the multiplicative noise correlation time τ_1, the correlation time τ_2 of the coupling between two noise terms, and the noise coupling strength λ, respectively.

Figures 2(a) and 2(b) are plots of the SNR when the multiplicative noise correlation time τ_1 is changed. For the initial condition $x(0)=x_+$ shown in Fig. 2(a), it is seen that the SNR is changed from one peak to two peaks when the value of τ_1 is increased. For small values of τ_1, there is only one peak in the SNR. When the value of τ_1 is increased, there appear two peaks in the SNR. When the value of τ_1 is increased further, the number of peaks in the SNR is reduced to one peak again. The height of the peaks is increased, while τ_1 is increased. For the initial condition $x(0)=x_-$ shown in Fig. 2(b), a similar phenomenon appears. However, the curves of the SNR for $x(0)=x_-$ are higher than those for

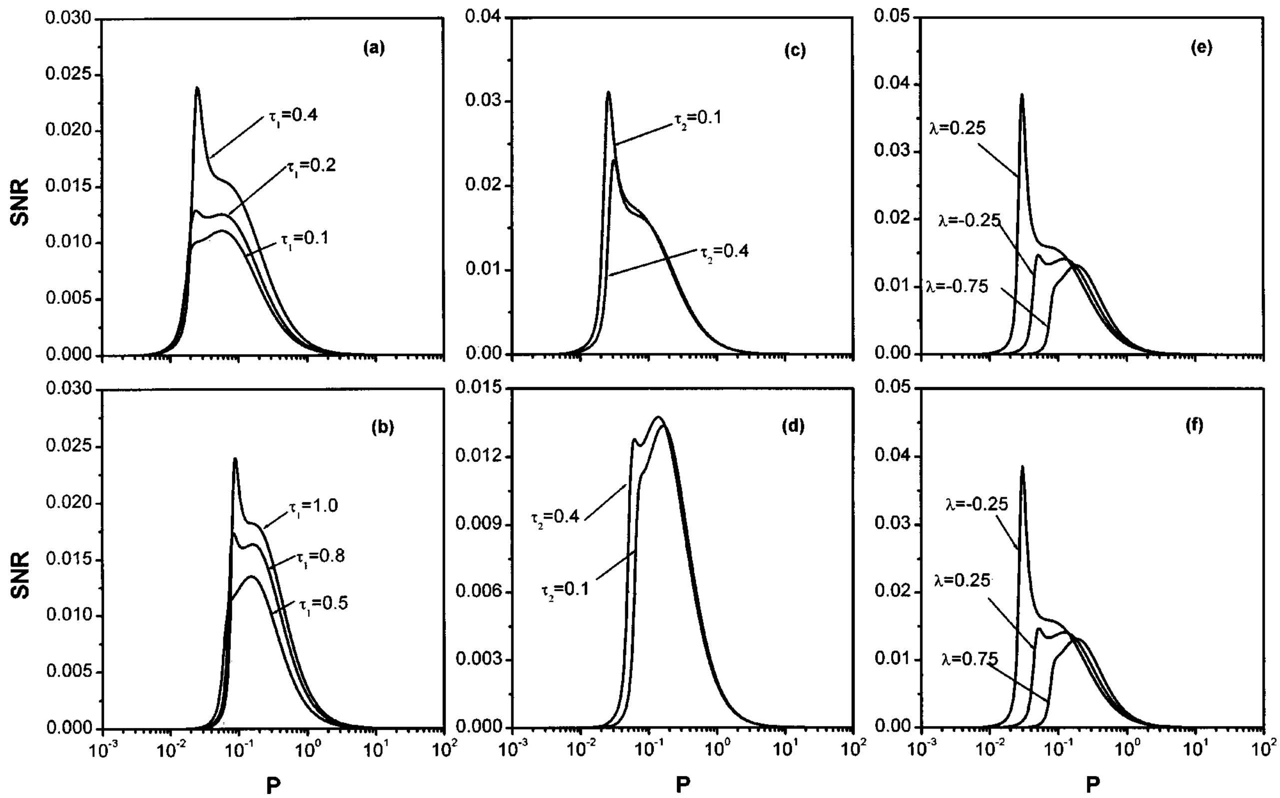

FIG. 3. Signal-to-noise ratio is as a function of the additive noise intensity P. The parameters are chosen as $P'=0.08$ and $\varepsilon=0.05$. All parameters are dimensionless. (a), (c), and (e) The initial condition is $x(0)=x_+$. (b), (d), and (f) The initial condition is $x(0)=x_-$. (a) and (b) The values of the multiplicative noise correlation time τ_1 are different with $\lambda=0.5$, $\tau_2=0.2$, and $\Omega=0.0013$. (c) and (d) The values of the correlation time τ_2 of the coupling between two noise terms are different with $\lambda=0.5$ and $\tau_1=0.5$. (c) $\Omega=0.0015$. (d) $\Omega=0.001$. (e) and (f) The values of the coupling strength λ are different with $\tau_1=0.5$, $\tau_2=0.2$, and $\Omega=0.001$.

$x(0)=x_+$. The shapes of the SNR for $x(0)=x_-$ are narrower than those for $x(0)=x_+$. From Figs. 2(a) and 2(b), it is clear that the correlation time τ_1 of multiplicative noise can induce the transition from one peak to two peaks, and then to one peak again in SR.

Figures 2(c) and 2(d) are plots of the SNR when the correlation time τ_2 of the coupling between additive and multiplicative noise is changed. The multiplicative noise correlation time τ_1 is fixed at 0.5. For the initial condition $x(0)=x_+$ shown in Fig. 2(c), it is clear that the one-peak structure in the SNR is not changed when τ_2 is increased. The positions of the peaks are increased to large values of P'. The height of the peaks is increased as τ_2 is increased. However, for the initial condition $x(0)=x_-$ shown in Fig. 2(d), quite a different phenomenon appears. The curve of the SNR is changed from two peaks to one peak as τ_2 is increased. The height of the peaks is decreased as the value of τ_2 is increased. The position of the peaks is changed to small values of P' as τ_2 is increased. From Figs. 2(c) and 2(d), it is clear that the correlation time τ_2 of the coupling between two noise terms can shift the position and change the height of the SNR. The effect of τ_2 on the number of peaks in the SNR depends on the initial condition of the system.

Figures 2(e) and 2(f) are plots of the SNR when the coupling strength λ between additive and multiplicative noise is changed. For initial condition $x(0)=x_+$ shown in Fig. 2(e), it is seen that the curve of the SNR is changed from one peak to two peaks, and then to one peak again when λ is reduced from zero to -0.8. For $\lambda=-0.8$, the peak of the SNR is very sharp. Figure 2(f) is a plot of the SNR for the initial condition $x(0)=x_-$. The curve is the same as that in Fig. 2(e), while the sign of λ is opposite to that in Fig. 1(e). That is, the curve of the SNR is changed from one peak to two peaks, and then to one peak again as λ is increased from zero to 0.8. The curve of $\lambda=0.8$ in Fig. 2(f) is the same as that of $\lambda=-0.8$ in Fig. 2(e). From Eqs. (19)–(21), it is found that the case of $\lambda>0$ with initial condition $x(0)=x_\pm$ equals that of $\lambda<0$ with $x(0)=x_\mp$.

B. Additive noise

The SNR as a function of the additive noise intensity P is plotted in Fig. 3 for different values of τ_1, τ_2, and λ, respectively.

Figures 3(a) and 3(b) are plots of the SNR when the multiplicative noise correlation time τ_1 is varied. For the initial condition $x(0)=x_+$ shown in Fig. 3(a), it is seen that the SNR is changed from one peak to two peaks, and then to one peak again when the value of τ_1 is increased. A similar phenomenon appears for the initial condition $x(0)=x_-$ shown in Fig. 3(b). It is seen that the two-peak structure appears for relatively small values of τ_1 with the initial condition $x(0)=x_+$ while that appears for relatively large values of τ_1 with the initial condition $x(0)=x_-$.

Figures 3(c) and 3(d) are plots of the SNR when the correlation time τ_2 of the coupling between additive and multiplicative noise is changed. For the initial condition $x(0)=x_+$ shown in Fig. 3(c), it is seen that there is only one peak in the SNR. The height of the peak in the SNR is decreased, while the position of the peak is shifted to a large value of P when the value of τ_2 is increased. For relatively large values of P, the curves of the SNR are only changed a small amount when τ_2 is increased. For the initial condition $x(0)=x_-$ shown in Fig. 3(d), the SNR is changed from one peak to two peaks as the value of τ_2 is increased. The height of the peak in the SNR is increased, while the position of the peak is shifted to a small value of P when the value of τ_2 is increased.

Figures 3(e) and 3(f) are plots of the SNR when the coupling strength λ between additive and multiplicative noise is changed. It is clear that the SNR is changed from one peak to two peaks, and then to one peak again when the value of the coupling strength λ is varied. For the initial condition $x(0)=x_+$ shown in Fig. 3(e), it is seen that the height of the curve is increased when λ is increased from -1 to $+1$. For the initial condition $x(0)=x_-$ shown in Fig. 3(f), all the behavior of the curve of the SNR is opposite to that in Fig. 3(e) for $x(0)=x_+$.

IV. COMPUTER SIMULATIONS AND DEPENDENCE OF INITIAL CONDITIONS

The computer simulations can be performed through Eq. (10), and the dependence of the SR on the initial conditions can be analyzed by Eq. (19).

A. Computer simulations

In order to check the range of validity of the approximation method employed in the derivation, it is necessary to perform computer simulations. The colored noise terms in Eq. (2) can be described by two differential equations of Ornstein-Uhlenbeck (OU) noise with constant intensity,

$$\frac{d\zeta_i(t)}{dt}=-\frac{\zeta_i(t)}{\tau_i}+\frac{\rho_i(t)}{\tau_i}\quad (i=1,2), \tag{22}$$

where $\rho_i(t)$ is Gaussian white noise with zero mean and

$$\langle\rho_i(t)\rho_j(t')\rangle=C_i\delta_{ij}\delta(t-t')\quad (i,j=1,2). \tag{23}$$

Here C_i is the strength of the corresponding colored noise.

The computer simulation is calculated by integrating the dynamical equations of motion, Eqs. (10), (22), and (23). Gaussian white noise is generated using the Box-Muller algorithm and a pseudo-random-number generator [44,45]. The numerical data of the time series are obtained using the Euler procedure. Then the data are calculated using a fast Fourier transform. To reduce the variance of the result, typically 1024 ensembles of power spectra, each containing 32 periods of the signal, are averaged. The output signal-to-noise ratio is defined as the ratio of the strength of the single peak to the mean amplitude of the background noise at the input signal frequency.

Since the spectral power amplification would allow an interpretation by time scale merging arguments and can be directly obtained from the peak of the power spectrum [5,16,29], the results of computer calculations of both the SNR and SPA are plotted in Fig. 4. The SNR are plotted in Figs. 4(a) and 4(c) as functions of multiplicative and additive noise strength P' and P, respectively. It is seen that the height of the curve of the SNR increases as the multiplicative noise correlation time τ_1 is increased. The curve of the SNR changes from one peak to two peaks, and then to one peak again as τ_1 is increased. Compared to Figs. 2 and 3, it is seen that there are longer tails in the computer calculations and sharper peaks in the analytic approximations. The computer simulations are performed over a wide range of the parameters ω, ε, τ_1, τ_2, and λ. Results similar to those in Figs. 4(a) and 4(c) are obtained. It is clear that the analytic results in the SNR shown in Figs. 2 and 3 are consistent with the computer simulations.

The values of the SPA as functions of P' and P are shown in Figs. 4(b) and 4(d), respectively. It is seen that the height of the SPA is increased as the multiplicative noise correlation time τ_1 is increased. The curve of the SPA also changes from one peak to two peaks, and then to one peak again as τ_1 is increased. Compared to that of the SNR, the curve of the SPA is much narrower than that of the SNR. The peaks of the SPA are also shifted to smaller values of P' and P. From Figs. 2–4, it seems that the noise color can both enhance the SR and induce two peaks in the SNR.

The two-peak structure in the SNR and SPA indicates the possibility that the periodic signals may be enhanced at two different values of the noise level instead of at a single value if the parameters in the stochastic system are changed.

B. Dependence of initial conditions

The standard SR, as it is classically defined with a periodic modulation, is essentially a steady-state property in the response of a nonlinear system. However, the SNR derived from Eqs. (10) and (19) depends on the initial condition $x(0)$. The SNR's of Eq. (19) as functions of multiplicative and additive noise strength P' and P are plotted in Figs. 5 and 6, respectively, when the coupling constant λ is changed with different initial conditions.

Figures 5(a)–5(d) are plots of the SNR as a function of P' when the coupling constant λ and two kinds of noise correlation time τ_1 and τ_2 are changed. The other parameters ω, ε, and P are fixed constants. From Fig. 5(a), it is seen that there is *no* dependence of the SNR on $x(0)$ for $\lambda=0$ even when $\tau_1=0.7$ and $\tau_2=0.2$. From Figs. 5(b)–5(d), it is seen that the curve of the SNR depends on the initial condition $x(0)$ when $\lambda=0.5$. For white noise with $\tau_1=\tau_2=0$, the peak of the SNR with $x(0)=x_+$ is higher than that with $x(0)=x_-$. The peak of the SNR is shifted to a smaller value of P' for $x(0)=x_+$ [Fig. 5(b)]. For colored noise with either $\tau_1=0.7$, $\tau_2=0$ or $\tau_1=0$, $\tau_2=0.2$, the peak of the SNR with $x(0)=x_+$ is lower than that with $x(0)=x_-$. The peak is also shifted to smaller values of P' [Figs. 5(c) and 5(d)].

Figures 6(a)–6(d) are plots of the SNR as a function of P when the coupling constant λ and two kinds of noise corre-

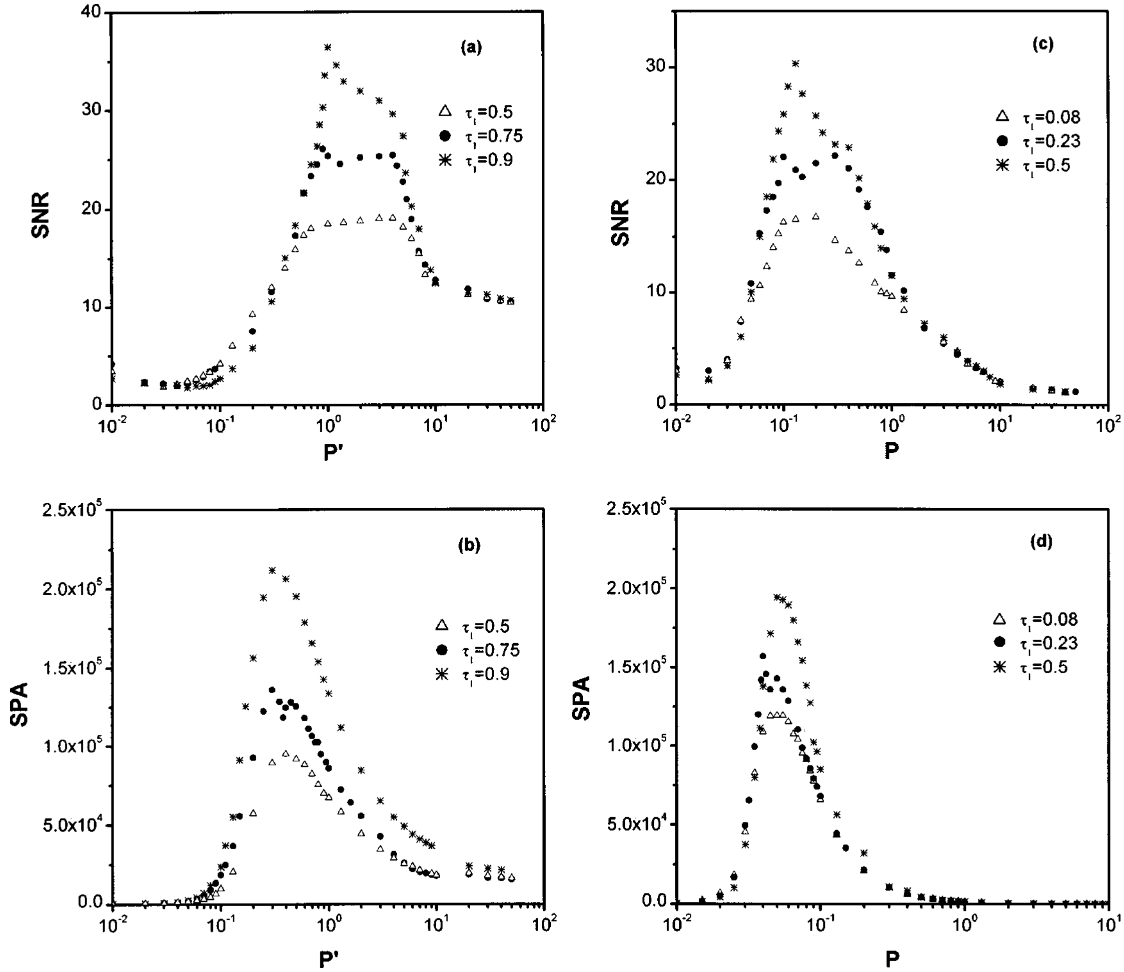

FIG. 4. Numerical simulations of the SNR and SPA as functions of the multiplicative and additive noise strength P' and P, respectively. The parameters are chosen as $x(0)=x_+$, $\varepsilon=0.05$, $\tau_2=0.2$, and $\lambda=0.5$. All parameters are dimensionless. (a) and (b) $\omega=0.003$ and $P=0.03$. △: $\tau_1=0.5$. ●: $\tau_1=0.75$. *: $\tau_1=0.9$. (c) and (d) $\omega=0.0015$ and $P'=0.08$. △: $\tau_1=0.08$. ●: $\tau_1=0.23$. *: $\tau_1=0.5$.

lation time τ_1 and τ_2 are changed. The other parameters ω, ε, and P' are fixed constants. From Fig. 6(a), it is seen that there is *no* dependence of the SNR on $x(0)$ for $\lambda=0$ even when $\tau_1=0.7$ and $\tau_2=0.2$. From Figs. 6(b)–6(d), it is seen that the curve of the SNR depends on the initial condition $x(0)$ in a similar manner with different height. The peak of the SNR with $x(0)=x_+$ is higher than that with $x(0)=x_-$. The peak of the SNR with $x(0)=x_+$ is shifted to a smaller value of P.

From Figs. 5 and 6, it is clear that the dependence of the SR on the initial condition $x(0)$ is entirely due to the coupling λ between two different kinds of noise terms.

V. TRANSITION BETWEEN ONE PEAK AND TWO PEAKS IN STOCHASTIC RESONANCE

The phenomenon of the transition between one peak and two peaks in stochastic resonance in the bistable nonlinear system, Eq. (1), can be analyzed by the number of maxima in the signal-to-noise ratio of Eq. (19).

A. Multiplicative noise

For multiplicative noise P', the maxima of the SNR can be determined by the equations $d(\mathcal{R})/dP'=0$ and $d^2(\mathcal{R})/d(P')^2<0$ from Eq. (19).

Figure 7 is a plot of the parameter planes τ_1-Ω, τ_2-Ω, and λ-Ω when the SNR is maximum as a function of the multiplicative noise intensity P'. In these figures, areas labeled "*S*" mean that there is a single peak in the SNR. Areas labeled "*T*" mean that there are two peaks in the SNR. Areas labeled "*N*" mean that there is no physical meaning in these parameter regimes since the SNR is less than zero.

Figures 7(a) and 7(b) are plots of the parameter plane τ_1-Ω of the multiplicative noise correlation time τ_1 and signal frequency Ω. For the initial condition $x(0)=x_+$ shown in Fig. 7(a), it is seen that the SNR is shifted between single peak and two peaks as the multiplicative noise correlation time τ_1 is increased. When the angular frequency Ω of the signal is in the region of $0.000\,14<\Omega<0.0014$, the SNR is changed from single peak to two peaks when τ_1 is increased. When Ω is in the region of $0.0014<\Omega<0.0040$, the SNR is shifted from single peak to two peaks, and then to single

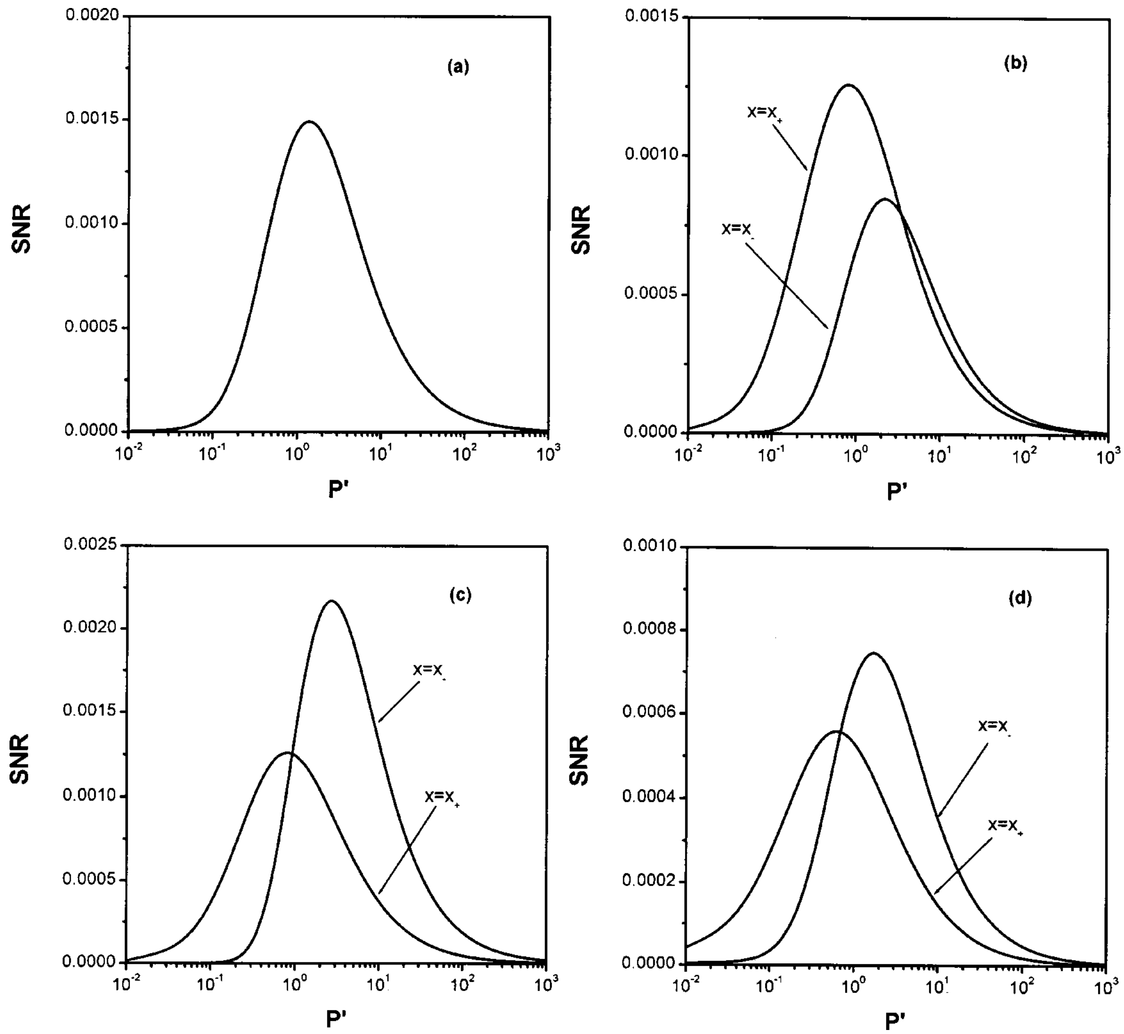

FIG. 5. SNR as a function of multiplicative noise strength P' when initial conditions are changed with different noise coupling constant λ. The parameters are chosen as $\omega=0.002$, $\varepsilon=0.01$, and $P=0.03$. All parameters are dimensionless. (a) $\lambda=0$, $\tau_1=0.7$, and $\tau_2=0.2$. (b) $\lambda=0.5$, $\tau_1=0$, and $\tau_2=0$. (c) $\lambda=0.5$, $\tau_1=0.7$, and $\tau_2=0$. (d) $\lambda=0.5$, $\tau_1=0$, and $\tau_2=0.2$.

peak again as τ_1 is increased. When Ω is in the region of $0.0040<\Omega$, there is only a single peak in the SNR as τ_1 is increased. When Ω is in the region of $\Omega<0.0023$, there is some region of no physical meaning in the SNR since a negative value of the SNR appears for these parameters. For the initial condition $x(0)=x_-$ shown in Fig. 4(b), a similar phenomenon appears. The transition between single peak and two peaks appears at smaller value of τ_1 than that for $x(0)=x_+$.

Figures 7(c) and 7(d) are plots of the parameter plane τ_2-Ω of the correlation time τ_2 of the coupling between additive and multiplicative noise and the signal frequency Ω. For the initial condition $x(0)=x_+$ shown in Fig. 7(c), there is no transition between single peak and two peaks as τ_2 is increased. When Ω is in the region of $0<\Omega<0.0007$, the region has no physical meaning in the SNR. When Ω is in the region of $0.0007<\Omega<0.0016$, there are two peaks in the SNR. When Ω is in the region of $0.0016<\Omega$, there is only a single peak in the SNR. In these regions, either a single peak or two peaks appears. There is no transition between the single peak and two peaks as τ_2 is increased. For the initial condition $x(0)=x_-$ shown in Fig. 7(d), it is seen that the SNR is shifted between single peak and two peaks. When Ω is in the region of $\Omega<0.0011$, the region of no physical meaning in the SNR appears. When Ω is in the region of $0.0011<\Omega<0.0019$, there are two peaks in the SNR and the two-peak structure in the SNR is not changed as τ_2 is increased. When Ω is in the region of $0.0019<\Omega<0.0031$, the SNR is changed from two peaks to a single peak as τ_2 is increased. When Ω is in the region of $0.0031<\Omega$, there is only a single peak in the SNR. It is clear that for the initial condition $x(0)=x_+$, the noise correlation time τ_2 cannot induce the transition between a single peak and two peaks in the SNR. However, for the initial condition $x(0)=x_-$, the noise correlation time τ_2 can induce a transition between a single peak and two peaks in the SNR. That is, the induced transition between single peak and two peaks by τ_2 also depends on the initial conditions.

Figures 7(e) and 7(f) are plots of the parameter plane λ-Ω of the coupling strength λ between additive and multiplica-

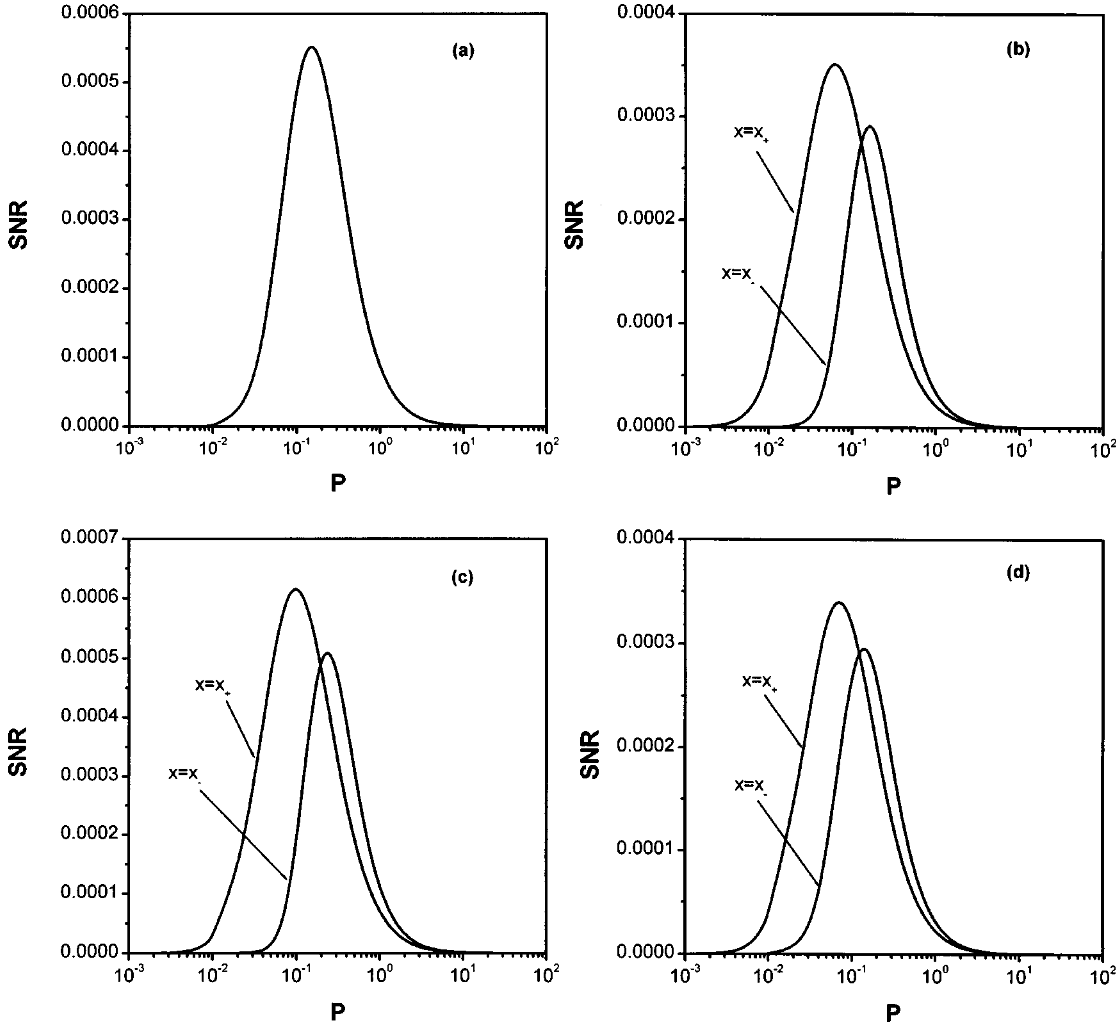

FIG. 6. SNR as a function of additive noise strength P when initial conditions are changed with different noise coupling constant λ. The parameters are chosen as $\omega=0.002$, $\varepsilon=0.01$, and $P'=0.08$. (a) $\lambda=0$, $\tau_1=0.7$, and $\tau_2=0.2$. (b) $\lambda=0.5$, $\tau_1=0$, and $\tau_2=0$. (c) $\lambda=0.5$, $\tau_1=0.7$, and $\tau_2=0$. (d) $\lambda=0.5$, $\tau_1=0$, and $\tau_2=0.2$.

tive noise and the signal frequency Ω. For the initial condition $x(0)=x_+$ shown in Fig. 7(e), the transition between single peak and two peaks appears in the SNR as λ is increased. When Ω is in the region of $\Omega<0.0006$, there exits an area of no physical meaning. When Ω is in the region of $0.0006<\Omega<0.0016$, there is a small area of no physical meaning. A two-peak structure appears in the SNR, and no transition between single peak and two peaks appears. When Ω is in the region of $0.0016<\Omega<0.0044$, the SNR is shifted from a single peak to two peaks and then to a single peak again as λ is increased. When Ω is in the region of $0.0044<\Omega$, there is only a single peak in the SNR as λ is increased. For the initial condition $x(0)=x_-$ shown in Fig. 7(f), a similar phenomenon appears. The transition between single peak and two peaks appears at a larger value of λ than that for $x(0)=x_+$ in Fig. 7(e). It seems that Fig. 4(f) is the result if Fig. 7(e) is rotated 180° along the axis of $\lambda=0$.

When the SNR is plotted as a function of the multiplicative noise strength P', it is seen that all of the parameters τ_1, τ_2, and λ can induce the transitions between a single peak and two peaks in SR.

B. Additive noise

For additive noise P, the maxima of the SNR can also be determined by the equations $d(\mathcal{R})/dP=0$ and $d^2(\mathcal{R})/dP^2<0$ from Eq. (19).

Figure 8 is a plot of the parameter planes τ_1-Ω, τ_2-Ω, and λ-Ω when the SNR is the maximum as a function of the additive noise intensity P. In these figures, the labels "*S*," "*T*," and "*N*" have the same meanings as that in Fig. 7.

Figures 8(a) and 8(b) are plots of the parameter plane τ_1-Ω of the multiplicative noise correlation time τ_1 and signal frequency Ω. For the initial condition $x(0)=x_+$ shown in Fig. 8(a), it is seen that the SNR is shifted between single peak and two peaks as the multiplicative noise correlation time τ_1 is increased. When the angular frequency Ω of the signal is in the region of $0.0005<\Omega<0.0008$, the SNR is changed from two peaks to a single peak when τ_1 is increased to 0.6. There is also an area of no physical meaning. When Ω is in the region of $0.0008<\Omega<0.002$, the SNR is shifted from a single peak to two peaks, and then to a single peak again as τ_1 is increased. When Ω is in the region of

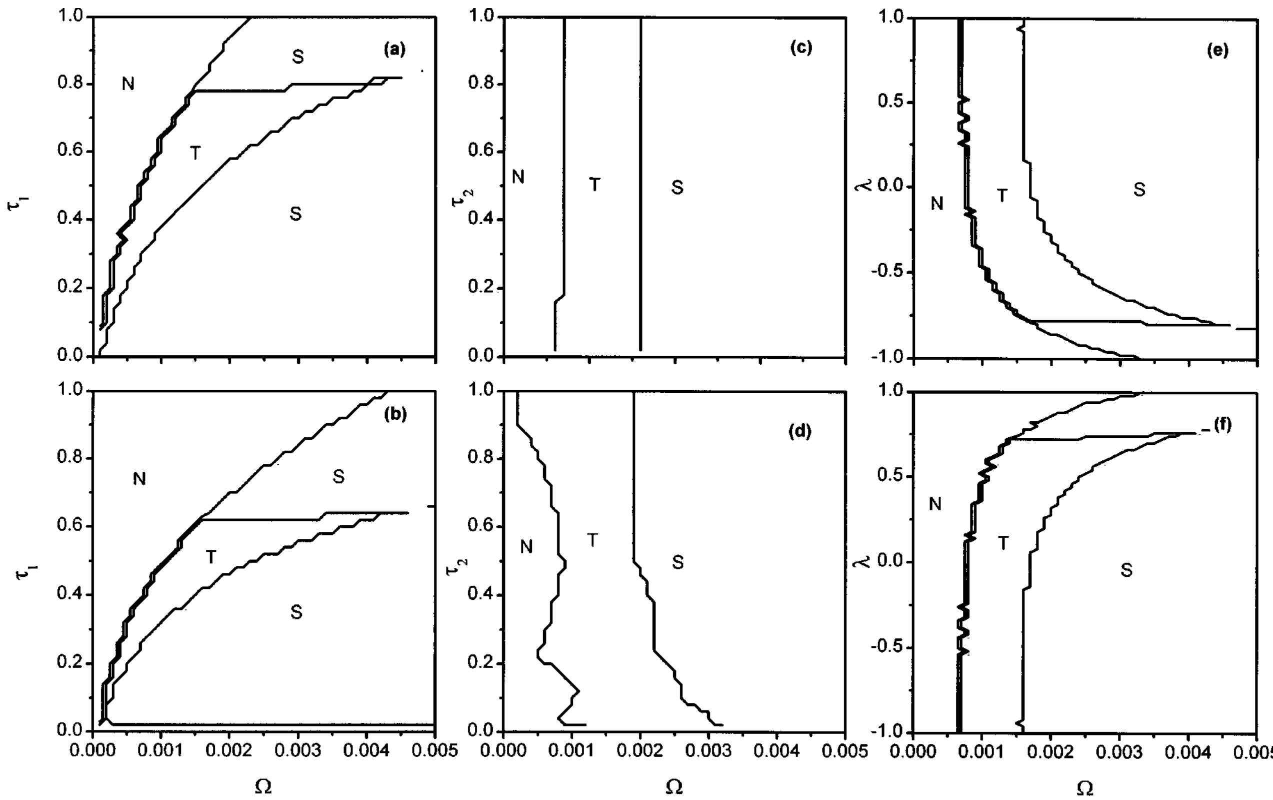

FIG. 7. Parameter planes as functions of the signal frequency Ω when the maximum of the SNR appears with respect to the multiplicative noise intensity P'. The parameters are chosen as $P=0.03$ and $\varepsilon=0.05$. The area labeled "S" means that there is a single peak in the SNR. Area labeled "T" means that there are two peaks in the SNR. The area labeled "N" means that there is no physical meaning in these parameter regimes since the SNR is less than zero. All parameters are dimensionless. (a), (c), and (e) The initial condition is $x(0)=x_+$. (b), (d), and (f) The initial condition is $x(0)=x_-$. (a) and (b) The parameter plane of τ_1-Ω with $\lambda=0.5$ and $\tau_2=0.2$. (c) and (d) The parameter plane of τ_2-Ω with (c) $\lambda=0.5$ and $\tau_1=0.5$ and (d) $\lambda=0.5$ and $\tau_1=0.2$. (e) and (f) The parameter plane of λ-Ω with $\tau_1=0.5$ and $\tau_2=0.2$.

$0.002<\Omega$, there is only a single peak in the SNR as τ_1 is increased. For the initial condition $x(0)=x_-$ shown in Fig. 8(b), a similar phenomenon appears with a different parameter regime. The transition between two peaks and a single peak appears at a larger value of τ_1 than that for $x(0)=x_+$.

Figures 8(c) and 8(d) are plots of the parameter plane τ_2-Ω of the correlation time τ_2 of the coupling between additive and multiplicative noise and the signal frequency Ω. For the initial condition $x(0)=x_+$ shown in Fig. 8(c), it is seen that except for the area of no physical meaning, there is only a single peak in the SNR no matter how τ_2 is changed. That is, there is no transition between single peak and two peaks as τ_2 is increased. For the initial condition $x(0)=x_-$ shown in Fig. 8(d), it is seen that the SNR is shifted between single peak and two peaks as τ_2 is increased. When Ω is in the region of $\Omega<0.000\,25$, there exists a region of no physical meaning in the SNR. When Ω is in the region of $0.000\,25<\Omega<0.0008$, there are two peaks in the SNR and no transition happens in the SNR as τ_2 is increased. When Ω is in the region of $0.0008<\Omega<0.0013$, the SNR is changed from a single peak to two peaks as τ_2 is increased. When Ω is in the region of $0.0013<\Omega$, only a single peak appears in the SNR as τ_2 is increased.

Figures 8(e) and 8(f) are plots of the parameter plane λ-Ω of the coupling strength λ between additive and multiplicative noise and the signal frequency Ω. For the initial condition $x(0)=x_+$ shown in Fig. 8(e), it is seen that the transition between a single peak and two peaks appears in the SNR as λ is increased. When Ω is in the region of $\Omega<0.0006$, there exists a region of no physical meaning and an area of two peaks in the SNR. There is no transition in the SNR. When Ω is in the region of $0.0006<\Omega<0.0023$, the SNR is shifted from a single peak to two peaks and then to a single peak again as λ is increased. When Ω is in the region of $0.0023<\Omega$, there is only a single peak in the SNR and no transition appears as λ is increased. For the initial condition $x(0)=x_-$ shown in Fig. 8(f), a similar phenomenon appears. The transition between a single peak and two peaks appears at a smaller value of λ than that for $x(0)=x_+$ in Fig. 8(e).

It is very interesting to note that the boundaries in the parameter space of Figs. 7 and 8 are not smooth curves. These figures, are checked by different calculations from derivations of Eq. (19). It seems that the zigzaglike boundaries shown in Figs. 7 and 8 are due to the small jumps of the parameters when the SNR is shifted between the regime of one peak and two peaks.

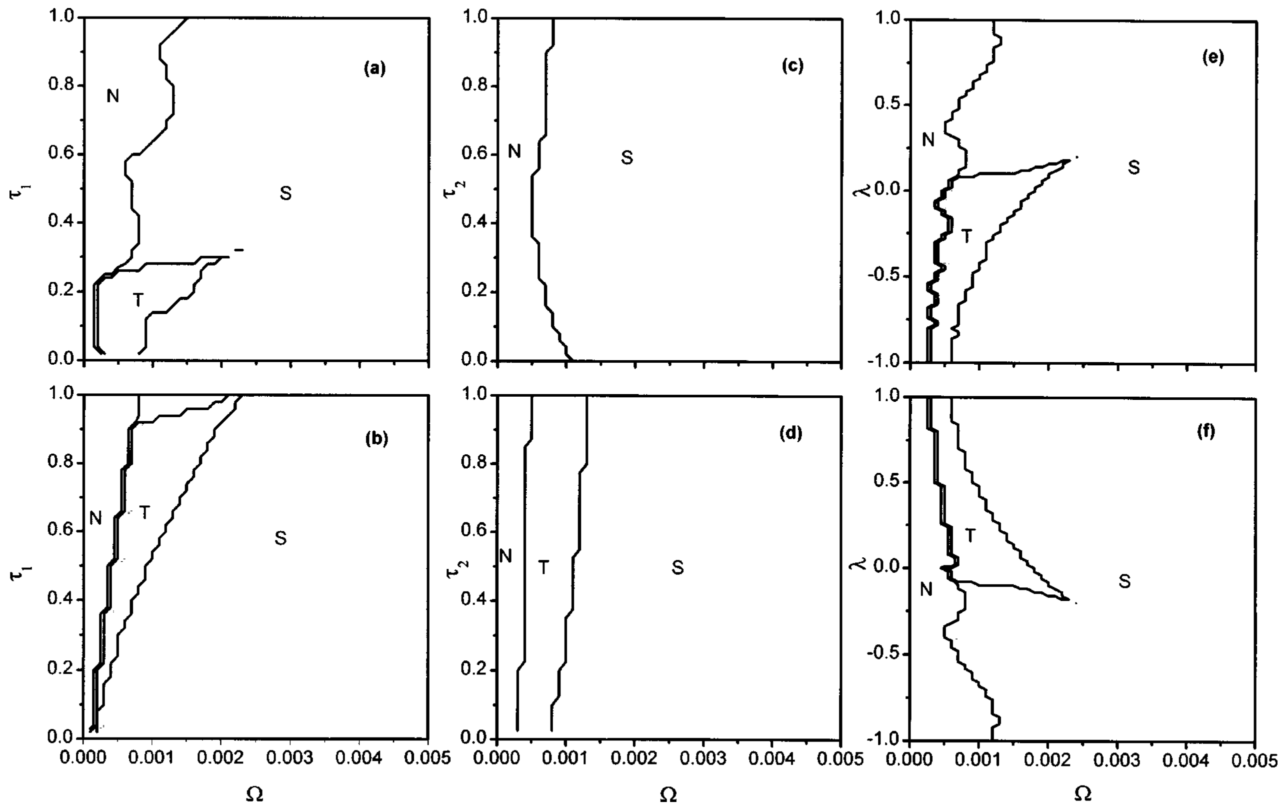

FIG. 8. Parameter planes as functions of the signal frequency Ω when the maximum of the SNR appears with respect to the additive noise intensity P. The parameters are chosen as $P'=0.08$ and $\varepsilon=0.05$. The area labeled "S" means that there is a single peak in the SNR. The area labeled "T" means that there are two peaks in the SNR. The area labeled "N" means that there is no physical meaning in these parameter regimes since the SNR is less than zero. All parameters are dimensionless. (a), (c), and (e) The initial condition is $x(0)=x_+$. (b), (d), and (f) The initial condition is $x(0)=x_-$. (a) and (b) The parameter plane of τ_1-Ω with $\lambda=0.5$ and $\tau_2=0.2$. (c) and (d) The parameter plane of τ_2-Ω with $\tau_1=0.5$ and $\lambda=0.5$. (e) and (f) The parameter plane of λ-Ω with $\tau_1=0.5$ and $\tau_2=0.2$.

VI. DISCUSSION

The stochastic resonance phenomenon in a bistable system driven by a weak periodic signal is investigated when the multiplicative colored noise and additive white noise are coupled with colored coupling between two noise terms. Appling the method of UCNA, the general stationary distribution function is derived. Through Fox's approach, the quasi-steady-state distribution function of the bistable system with a periodic signal is obtained in the adiabatic limit. Then by virtue of the two-state approach, the expression of the SNR is derived.

The effects of multiplicative colored noise correlation time τ_1, the correlation time τ_2 of the coupling between two noise terms, and the coupling strength λ on the SNR are investigated. It is found that all parameters τ_1, τ_2, and λ can induce the transition between one peak and two peaks in the curve of the SNR. When the values of τ_1 and λ are increased, there appears a transition from one peak to two peaks, and then from two peaks to one peak again. The transition between one peak and two peaks does not depend on the initial condition $x(0)$ of the system. When the value of τ_2 is increased, there appears a transition either from one peak to two peaks or from two peaks to one peak. There does not appear the phenomenon of the transition from one peak to two peaks, and then to one peak again. The transition between one peak and two peaks also depends on the initial condition of $x(0)$. For certain initial conditions, there may be no transition between one peak and two peaks. It seems that the transition between one peak and two peaks induced by τ_1 and λ is more complex than that induced by τ_2.

The phenomenon of multiple peaks in the SNR or SPA has also been found in Refs. [3], [26], and [29] for different models. It seems that the two peaks in the SNR in the pioneering paper [3] is mainly due to the feedback of the noise into the signal causing a dip in the SNR at very small signal frequency. The multiple peaks in the SNR can be caused by either periodic or multiple maxima and minima in the potential [26]. The two peaks in the SNR and SPA can be induced by dichotomic noise in a bistable system [29]. In this paper, the two-peak structures in the SNR and SPA are mainly induced by the multiplicative noise correlation time τ_1, the correlation time τ_2, and strength λ of the coupling between two noise terms.

It is seen that both the height and number of peaks in the SNR and SPA can be varied if the parameters τ_1, τ_2, and λ are changed. This may provide another possibility of controlling stochastic resonance. The SR can be either enhanced or suppressed, and the number of peaks in the SR can also be increased or decreased by changing the parameters. So far the control of the SR is investigated theoretically and experimentally when upper and lower barriers of either a threshold or potential energy barrier are modulated [34–37].

ACKNOWLEDGMENTS

It is a pleasure to thank Professor Yinsheng Ling for his many helpful discussions of colored noise. Financial support from the National Natural Science Foundation of China (Grant No. 19874046) and the Natural Science Foundation of Jiangsu Province (Grant No. BK 2001138) is gratefully acknowledged.

[1] R. Benzi, A. Sutera, and A. Vulpiani, J. Phys. A **14**, L453 (1981).
[2] R. Benzi, G. Parisi, A. Sutera, and A. Vulpiani, Tellus **34**, 10 (1982).
[3] B. McNamara and K. Wiesenfeld, Phys. Rev. A **39**, 4854 (1989).
[4] T. Zhou and F. Moss, Phys. Rev. A **41**, 4255 (1990).
[5] P. Jung and P. Hänggi, Phys. Rev. A **44**, 8032 (1991).
[6] G. Hu, G. R. Qing, D. C. Gong, and X. D. Weng, Phys. Rev. A **44**, 6414 (1991).
[7] G. Hu, T. Ditzinger, C. Z. Ning, and H. Haken, Phys. Rev. Lett. **71**, 807 (1993).
[8] M. I. Dykman, R. Mannella, P. V. E. McClintock, and N. G. Stocks, Phys. Rev. Lett. **68**, 2985 (1992).
[9] A. Neiman and L. Schimansky-Geier, Phys. Rev. Lett. **72**, 2988 (1994).
[10] P. Jung and G. Maye-Kress, Phys. Rev. Lett. **74**, 2130 (1995).
[11] L. Gamma, F. Marchesoni, and S. Santucci, Phys. Rev. Lett. **74**, 1052 (1995).
[12] W. Yang, M. Ding, and G. Hu, Phys. Rev. Lett. **74**, 3955 (1995).
[13] J. F. Lindner, B. K. Meadows, W. L. Ditto, M. E. Inchiosa, and A. R. Bulsara, Phys. Rev. Lett. **75**, 3 (1995).
[14] G. Hu, H. Haken, and F. Xie, Phys. Rev. Lett. **77**, 1925 (1996).
[15] A. R. Bulsara and L. Gammaitoni, Phys. Today **49** (3), 39 (1996).
[16] L. Gammaitoni, P. Hanggi, P. Jung, and F. Marchesoni, Rev. Mod. Phys. **70**, 224 (1998).
[17] V. Berdichevsky and M. Gitterman, Phys. Rev. E **60**, 1494 (1999).
[18] F. Marchesoni, F. Apostolico, and S. Santucci, Phys. Rev. E **59**, 3958 (1999).
[19] M. M. Alibegov, Phys. Rev. E **59**, 4841 (1999).
[20] Y. Jia, S. Yu, and J. Li, Phys. Rev. E **62**, 1869 (2000).
[21] C. J. Tessone, H. S. Wio, and P. Hanggi, Phys. Rev. E **62**, 4623 (2000).
[22] Y. Jia, X. Zheng, X. Hu, and J. Li, Phys. Rev. E **63**, 031107 (2001).
[23] H. E. Plesser and T. Geisel, Phys. Rev. E **63**, 031916 (2001).
[24] A. A. Zaikin, J. Kurths, and L. Schimansky-Geier, Phys. Rev. Lett. **85**, 227 (2000).
[25] A. A. Zaikin, K. Murali, and J. Kurths, Phys. Rev. E **63**, 020103 (2001).
[26] J. M. G. Vilar and J. M. Rubi, Phys. Rev. Lett. **78**, 2882 (1997).
[27] J. M. G. Vilar and J. M. Rubi, Phys. Rev. Lett. **78**, 2886 (1997).
[28] J. M. G. Vilar, G. Gomula, and J. M. Rubi, Phys. Rev. Lett. **81**, 14 (1998).
[29] R. Rozenfeld, A. Neiman, and L. Schimansky-Geier, Phys. Rev. E **62**, R3031 (2000).
[30] R. Rozenfeld, J. A. Freund, A. Neiman, and L. Schimansky-Geier, Phys. Rev. E **64**, 051107 (2001).
[31] I. Goychuk and P. Hänggi, Phys. Rev. E **59**, 5137 (1999).
[32] N. G. Stocks, Phys. Rev. E **63**, 041114 (2001).
[33] N. G. Stocks, Phys. Lett. A **279**, 308 (2000).
[34] L. Gammaitoni, M. Locher, A. Bulsara, P. Hanggi, J. Neff, K. Wiesenfeld, W. Ditto, and M. E. Inchiosa, Phys. Rev. Lett. **82**, 4574 (1999).
[35] M. Locher, M. E. Inchiosa, J. Neff, A. Bulsara, K. Wiesenfeld, L. Gammaitoni, P. Hanggi, and W. Ditto, Phys. Rev. E **62**, 317 (2000).
[36] J. F. Lindner, J. Mason, J. Neff, B. J. Breen, W. L. Ditto, and A. R. Bulsara, Phys. Rev. E **63**, 041107 (2001).
[37] J. F. Lindner, B. J. Breen, M. E. Wills, A. R. Bulsara, and W. L. Ditto, Phys. Rev. E **63**, 051107 (2001).
[38] I. I. Fedchenia, J. Stat. Phys. **52**, 1005 (1988).
[39] A. Fulinski and T. Telejko, Phys. Lett. A **152**, 11 (1991).
[40] P. Hanggi and P. Jung, Adv. Chem. Phys. **89**, 239 (1995).
[41] Cao Li, Wu Da-jin, and Ke Sheng-zhi, Phys. Rev. E **52**, 3228 (1995).
[42] R. F. Fox, Phys. Rev. A **34**, 4525 (1986).
[43] Y. Jia and J. Li, Phys. Rev. E **53**, 5786 (1996).
[44] R. F. Fox, I. R. Gatland, R. Roy, and G. Vemuri, Phys. Rev. A **38**, 5938 (1988).
[45] W. H. Press, S. A. Teukolsky, W. T. Vetterling, and B. P. Flannery, *Numerical Recipes in FORTRAN*, 2nd ed. (Cambridge University Press, Cambridge, England, 1992).